Available online at www.sciencedirect.com
ScienceDirect
Geochimica et Cosmochimica Acta 71 (2007) 3887–3903
Geochimica et Cosmochimica Acta
www.elsevier.com/locate/gca

Zircons from kimberlite: New insights from oxygen isotopes, trace elements, and Ti in zircon thermometry

F. Zeb Page [a,*], Bin Fu [a], Noriko T. Kita [a], John Fournelle [a], Michael J. Spicuzza [a], Daniel J. Schulze [b], Fanus Viljoen [c], Miguel A.S. Basei [d], John W. Valley [a]

[a] Department of Geology & Geophysics, University of Wisconsin-Madison, 1215 W. Dayton St., Madison, WI 53706, USA
[b] Department of Geology, University of Toronto, Erindale College, Mississauga, Ont., L5L 1C6, Canada
[c] Geoscience Centre, De Beers Consolidated Mines Ltd., P.O. Box 82232, Southdale 2135, South Africa
[d] Department of Geosciences, University of São Paulo, 05508-080 São Paulo, SP, Brazil

Received 8 May 2006; accepted in revised form 23 April 2007; available online 21 May 2007

Abstract

Zircons found in mantle-sourced kimberlite provide probes into the isotopic chemistry of the asthenosphere and subcontinental lithospheric mantle. However, little is known about the conditions of formation of these zircons. A suite of 88 zircons found in kimberlites from Africa, Siberia, Brazil, and the United States have been analyzed for their Ti concentration and selected zircons were analyzed for their Rare Earth Element (REE) concentrations by ion microprobe. In addition, precise and accurate laser-fluorination oxygen isotope data were obtained for zircons from Brazil ($5.1 \pm 0.3‰$, 1SD) and the Midwest United States ($5.3 \pm 0.3‰$), yielding mantle-like $\delta^{18}O$ values similar to published data for Africa ($5.2 \pm 0.3‰$) and Siberia ($5.3 \pm 0.2‰$). Most megacrysts in this study preserve fine-scale, oscillatory zoning in CL and are generally homogenous in oxygen isotopic composition, consistent with preservation of primary compositions. A few zircons from Brazil show some evidence of chemical zoning due to recrystallization. The Ti content of mantle zircon is in general low with average compositions from each locality of 13 ± 8.4 ppm (1SD, Kaapvaal craton), 12 ± 8.7 ppm (Siberian platform), 18 ± 11 ppm (Brazil), and 4.8 ± 4.3 ppm (United States). The recently calibrated Ti in zircon thermometer yields an average temperature of 744 ± 62 °C (1SD) for the average of 13 ± 9 ppm Ti, with no correction for pressure, a_{TiO_2}, or a_{SiO_2}. The Ti content of zircons found within rutile nodules from the Orapa kimberlite (Kaapvaal craton) is almost indistinguishable from those with no constraint on a_{TiO_2}, suggesting that reduced a_{TiO_2} is not responsible for lower than expected mantle temperatures. The average temperature in this study corresponds to ~3 GPa on a 40 mW/m^2 cratonic geotherm. If correct, this would suggest that zircon megacrysts from all four cratons formed in the shallow lithospheric mantle. However, there are several possibly confounding effects to this thermometer, including: a pressure correction and disequilibrium zircon growth. Zircons from rutile nodules have REE contents that span the range of mantle zircon REE and are similar to both zircon megacrysts and zircons from metasomatic assemblages.

1. INTRODUCTION

Zircon is an almost ubiquitous trace mineral in most igneous and metamorphic rocks, and is widely studied because it preserves a robust record of magmatic oxygen isotope ratio (Valley, 2003), trace element content, and U–Th–Pb isotopic chemistry (Hanchar and Hoskin, 2003). Because of its refractory nature, zircon is often preserved as a xenocryst or detrital grain after the destruction of its original host. Xenocrystic or detrital zircon is found as detritus in (meta)sedimentary rocks or as an inherited phase within igneous rocks, and is generally similar in size (<500 μm) to the zircons common in most igneous and metamorphic rocks.

One enigmatic occurrence of zircon is as megacrysts of up to cm-size hosted by mantle-sourced kimberlite.

* Corresponding author. Present address: Geology Department, Oberlin College, 52 W. Lorain St., Oberlin, OH 44074, USA. Fax: +1 440 775 8038.
E-mail address: zeb.page@oberlin.edu (F.Z. Page).

0016-7037/$ - see front matter © 2007 Elsevier Ltd. All rights reserved.
doi:10.1016/j.gca.2007.04.031

Textural, chemical, mineral inclusion, and oxygen isotopic data suggest that many zircons found in kimberlite are the products of the mantle, as opposed to crustal zircons sampled by the kimberlite during eruption (e.g., Kresten et al., 1975; Gurney et al., 1979; Belousova et al., 1998; Valley et al., 1998). These zircons either formed from melts or metasomatic fluids (e.g., Spetsius et al., 2002) within the mantle. However, little is known about the conditions of formation of these unusual crystals other than their mantle association.

A great deal of effort has been applied to extract petrologic information from the trace element composition of zircon in the absence of its original host rock. A recent, and potentially powerful, addition to the suite of tools used in the study of zircon is the use of the Ti content of zircon as an indicator of crystallization temperature (Watson and Harrison, 2005). This study presents analyses of Ti from mantle megacryst zircon from southern Africa and Siberia (Figs. 1 and 2) previously analyzed for oxygen isotopes by Valley et al. (1998). In addition, oxygen isotope and Ti data from zircon megacrysts from Brazil (Fig. 3) and the United States and Rare Earth Element (REE) data from selected zircons from all four localities are presented. Titanium thermometry of individual zircons may allow us to put better constraints on the conditions of zircon megacryst formation, whereas the addition of new REE and oxygen isotope data shows subtle geochemical variability from the intracrystalline to intercontinental scale.

2. ZIRCONS IN KIMBERLITE

Zircons are found in kimberlite within xenoliths of both crustal (e.g., Schmitz and Bowring, 2003) and mantle (e.g., Konzett et al., 2000) origin. Zircon is also found as individual crystals (often megacrystic) within kimberlite at the ppm level that are concentrated with diamonds during mining. These zircons are texturally quite distinct from crustal zircons: they are generally large (mm to cm size), rounded, clear, gemmy, and show distinct cleavage or parting (Kresten et al., 1975). These megacrysts commonly display the oscillatory zoning in cathodoluminescence (CL) imaging typical of igneous zircon (Fig. 4). This zoning is commonly truncated at grain margins that have altered to tetragonal ZrO_2 or baddeleyite (Fig. 4b; Corfu et al., 2003). Zircon megacrysts from kimberlite also have a trace element composition that is distinctive from crustal zircons with low U (<60 ppm) and a flat chondrite-normalized heavy rare earth element (HREE) pattern significantly less enriched than crustal zircons (Belousova et al., 1998; Hoskin and Ireland, 2000; Belousova et al., 2002). Although, in a few notable cases, the U–Pb ages of some zircon megacrysts predate the eruption age of the host kimberlite (e.g., Kinny et al., 1989; Belousova et al., 2001; Zartman and Richardson, 2005), in most cases, zircon megacrysts record the time of kimberlite eruption, either because of contemporaneous formation, or cooling below the closure temperature of Pb in zircon (e.g., Davis et al., 1980; Kinny et al., 1995; Zartman and Richardson, 2005).

2.1. Paragenesis

The paragenesis of zircon in kimberlite remains uncertain. Gurney et al. (1979) assigned zircon megacrysts from the Monastery kimberlite (South Africa) to the Cr-poor megacryst suite (olivine, clinopyroxene, orthopyroxene, garnet, ilmenite, and phlogopite). This suite of megacrysts has been shown to be genetically related to the host kimberlite by radiogenic isotopes (Smith et al., 1995), and is thought to consist of deep-seated liquidus phases. The major and trace element chemistry of these megacrysts record fractional crystallization (e.g., Gurney et al., 1979; Moore, 1992) and possibly some interaction between the megacryst host magma and

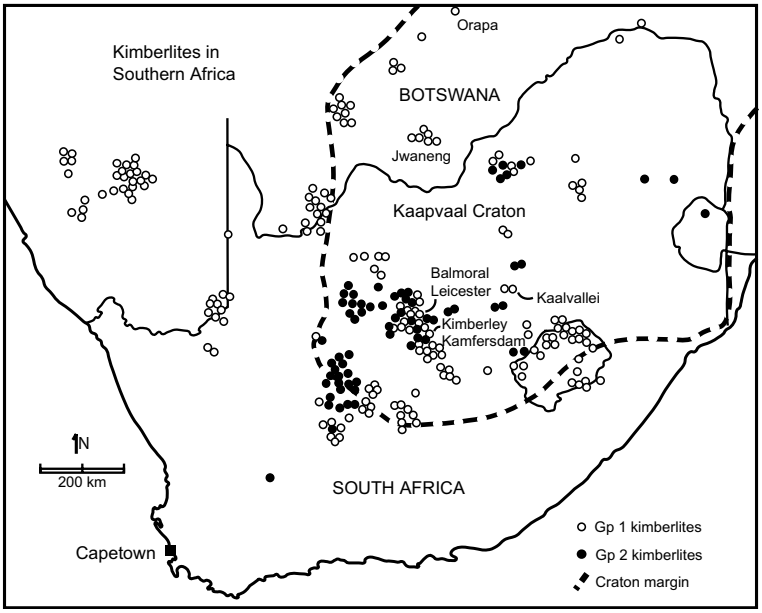

Fig. 1. Map of kimberlite pipes from southern Africa (after Skinner, 1989). Zircons from the labeled group 1 kimberlites were analyzed for Ti by ion microprobe in this study, and selected zircons from each locality were analyzed for REE. Oxygen isotopic compositions of zircons from these localities were reported by Valley et al. (1998). The Leicester kimberlite is adjacent to Balmoral, and Kamfersdam is in Kimberley.

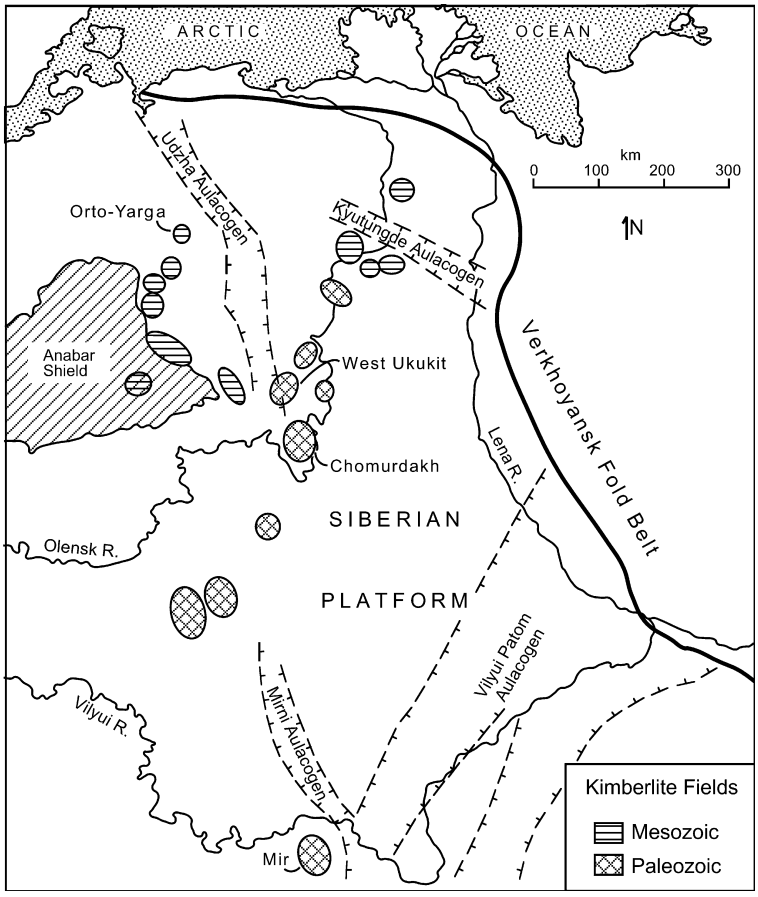

Fig. 2. Map of the Siberian platform showing kimberlite fields. Zircons from the labeled fields were analyzed for Ti and REE by ion microprobe. Oxygen isotopic compositions of zircons from these localities were reported by Valley et al. (1998).

Fig. 3. Map of Brazil showing the Juina and Alto Paranaiba kimberlite provinces and approximate boundaries of cratons. Zircons from kimberlite pipes from both fields were analyzed for $\delta^{18}O$ by laser fluorination and for Ti content by ion microprobe. Zircons from two pipes from each field were analyzed for REE by ion microprobe.

the subcontinental lithospheric mantle (SCLM; e.g., Moore, 1992; Bell and Moore, 2004). However, the link between zircon as a late liquidus phase and the earlier-formed minerals of the suite is purely based on size and not on chemistry and is therefore tenuous. Some zircon megacrysts (from the Balmoral and Leicester kimberlites) have been found intergrown with Cr-rich diopside, rutile, and ilmenite, suggesting a relation to the "Granny Smith-like" association (Boyd et al., 1984). Megacrysts from the Kamfersdam kimberlite have been found intergrown with K-richterite, clinopyroxene, phlogopite, and ilmenite, suggesting a relation to the MARID (mica–amphibole–rutile–ilmenite–diopside) and PKP (phlogopite-K-richterite-peridotite) metasomatic assemblages (Dawson and Smith, 1977; Kinny and Dawson, 1992). Zircons from the Mir kimberlite (Siberia) contain inclusions of chromite, Cr-rich diopside, forsterite, Ni-rich sulfide and phlogopite, and have been interpreted as having grown during the metasomatism of peridotite (Spetsius et al., 2002). Some zircons found in MARID and other metasomatic associations can be distinguished from megacrystic zircon because of higher U and Th content (Davis, 1977; Konzett et al., 1998; Dawson et al., 2001). However, zircons from metasomatic xenoliths have also been found with similar textural and trace element characteristics to zircon megacrysts (Konzett et al., 2000).

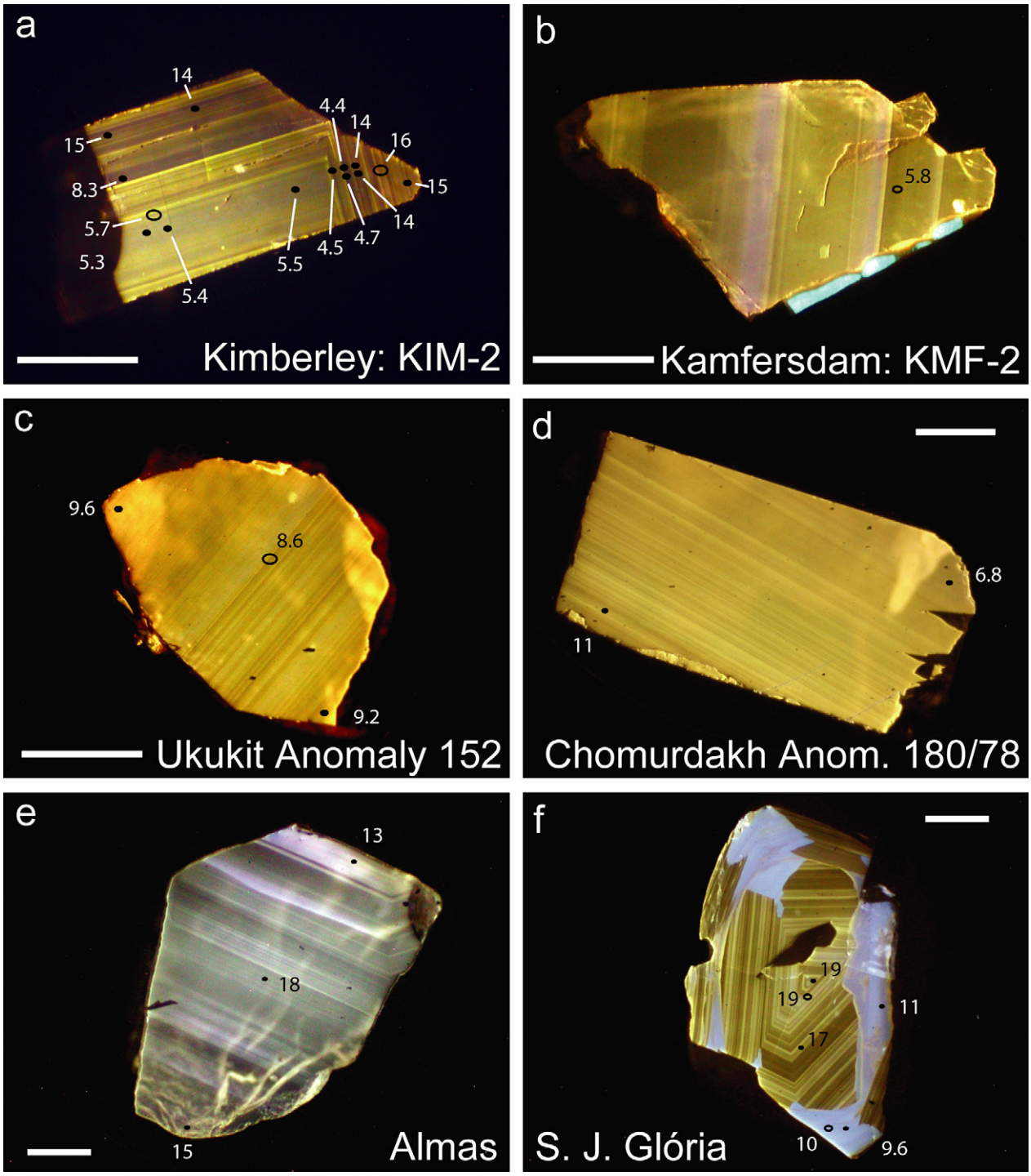

Fig. 4. Cathodoluminesence images of fragments from zircon megacrysts. Filled ellipses represent Ti ion microprobe analyses, open ellipses represent Ti + REE analyses, Ti is indicated in ppm. The highly CL-active rim on the lower-right of the crystal in (b) is the ZrO_2 reaction rim at the edge of the zircon that truncates growth zoning. Scale bars are 250 μm.

2.2. Sensors of mantle processes

Despite varied and uncertain parageneses, the geochemistry of zircon (and other) megacrysts has been used to offer insight into mantle reservoirs and the processes of kimberlite formation. Valley et al. (1998) showed that zircon megacrysts record a narrow range of oxygen isotope composition (average $\delta^{18}O_{VSMOW} = 5.3 \pm 0.3‰$, 1SD) in equilibrium with common mantle values, but that subtle pipe to pipe variations may record distinct mantle reservoirs in the asthenospheric mantle or the SCLM. Oxygen isotopes from low-Cr garnet megacrysts found in Group I kimberlites (Rb/Sr and Sm/Nd similar to bulk earth; Smith, 1983) record similar, restricted compositions typical of the mantle

($\delta^{18}O = 5.24 \pm 0.15‰$, 1SD), whereas similar garnet megacrysts from Group II kimberlites (depleted mantle source, e.g., SCLM) are anomalously enriched in $\delta^{18}O$ ($5.59 \pm 0.18‰$, 1SD; Schulze et al., 2001). These mildly elevated values are likely to have resulted from assimilation of altered ocean crust that was subducted and incorporated into the SCLM prior to kimberlite formation.

The Hf isotopic composition of mantle zircons has been used as a sensor of the Hf systematics of the SCLM. Whereas, the Hf isotopic composition of many mantle zircons suggests that they formed from a variably depleted mantle source, some samples contain significantly less radiogenic Hf. This may record interaction with reservoirs of non-radiogenic Hf in the SCLM (Griffin et al., 2000). Because of limited overlap in the kimberlite pipes studied, it is not clear if heterogeneities in Hf and oxygen isotopic composition are correlated. Zartman and Richardson (2005) have argued for a secular decrease in the Th/U content of the mantle based on the Th and U composition of dated zircon megacrysts. It should be noted that in one of the two Precambrian suites (Jwaneng) upon which this assertion is based, zircons have a $\delta^{18}O$ range of 3.37–4.72‰ (VSMOW), significantly lower than well-mixed mantle values (Valley et al., 1998) and a different trace element composition than the majority of mantle zircons (Belousova et al., 2002), suggestive of a crustal origin.

2.3. Thermobarometry

Although zircons from kimberlite have been used to provide insight into the chemical and isotopic nature of various mantle reservoirs, little is known about their pressures and temperatures of formation. In igneous models of zircon formation, they are generally assigned to the Cr-poor megacryst suite (Gurney et al., 1979). Silicate megacrysts more amenable to thermobarometry than zircon (e.g., orthopyroxene, clinopyroxene) record high temperatures and pressures (1000–1400 °C, 4.5–5.5 GPa) suggesting crystallization in the asthenospheric mantle (Nixon and Boyd, 1973; Gurney et al., 1979; Schulze, 1987). However, if zircon actually belongs to the Cr-poor megacryst suite, it likely formed at the end of the fractional crystallization sequence in a late differentiated magma, for which crystallization temperatures are not known (Moore, 1992). The thermometry of zircons associated with metasomatic assemblages is equally poorly constrained. Thermometry of the MARID suite is essentially nonexistent because of the lack of minerals suited for thermobarometry (Zhao et al., 1999). Other metasomatic assemblages (e.g. PKP) may contain potential thermobarometers but disequilibrium textures between those minerals make P-T estimates (700–900°, 3.7 GPa) suspect (Konzett et al., 2000). The compositions of clinopyroxene inclusions in zircons from the Mir kimberlite have been used to estimate a temperature of 950 °C (Garanin et al., 1993; Spetsius et al., 2002). However, Spetsius et al. (2002) suggested that the inclusions predate the host zircon, and it is unclear if thermometry of inclusions is applicable to the zircon, or only to the host peridotite before metasomatism. Application of the Ti in zircon thermometer to kimberlite zircons may provide the first real insight into the temperatures of formation of these enigmatic crystals. A better understanding of the conditions of formation of zircon megacrysts will bolster their use as an important sensor of mantle geochemistry.

3. METHODS

3.1. Analysis of oxygen isotopes

Analysis of oxygen isotopes was performed on 1–2 mg zircon chips removed from larger megacrysts by hand crushing. Samples were laser heated in a BrF_5 atmosphere and analyzed using a dual-inlet gas-source mass spectrometer. Isotopic ratios are reported in per mil (‰) notation relative to standard mean ocean water (VSMOW). Accuracy and analytical precision was verified during each session by multiple analyses of the garnet standard UWG-2 (Valley et al., 1995). Raw $\delta^{18}O$ values of standard for each session were corrected to the accepted UWG-2 value ($\delta^{18}O = 5.80$ ‰) and the same correction was applied to samples. The average uncorrected $\delta^{18}O$ values (±1SD) of UWG-2 for three analysis sessions are 5.82 ± 0.01, $n = 3$; 5.78 ± 0.10, $n = 4$; 5.85 ± 0.06, $n = 4$; daily corrections were <0.05‰.

3.2. Analysis of titanium

Titanium was measured in kimberlite zircons alone and in conjunction with REE by ion microprobe using a CAMECA ims-1280 at the Department of Geology and Geophysics at the University of Wisconsin–Madison (WiscSIMS). A 4 nA O^- primary ion beam (23 keV total accelerating voltage) was shaped to a diameter of 25 μm on the sample surface, and positive secondary ions were accelerated by 10 kV. The configuration of the secondary ion optics was optimized for high transmission, similar to that found in Kita et al. (2004) for trace element analysis. However, modifications to that method include the use of narrower entrance and exit slit widths (75 μm and 200 μm, respectively) to achieve a higher mass resolving power (MRP) of ~4500 and the application of anisotropic "XY-mode" beam processing reducing aberrations in the transverse plane and thus tailing of the mass spectrum. Of the five isotopes of Ti (46, 47, 48, 49, and 50), the comparatively low abundance ^{49}Ti (5.5%) was used to analyze Ti concentration because of isobaric interference by intense doubly charged Zr peaks on ^{46}Ti, ^{47}Ti, and ^{48}Ti peaks, and possibly from ^{48}Ca and ^{50}Cr on ^{48}Ti and ^{50}Ti, respectively. No energy offset was applied because the MRP of 4500 was sufficient to eliminate any potential molecular isobaric interference on ^{49}Ti. A reduced field aperture (1000 μm square) was used to limit analysis to the central 5 μm square within the 25 μm sputtered pit. This configuration limits possible contamination by Ti from the sample surface, and is also effective in stabilizing relative Si and Ti ion yield, which significantly changes (as much as 30%) after the beginning of sample presputtering. Zircons were presputtered for 3 min before each analysis to eliminate Ti contamination and to stabilize the relative ion yield of $^{49}Ti/^{30}Si$. Analyses were conducted in monocollection mode

using electron multiplier pulse counting to measure $^{30}Si^{+}$ (1 s), $^{91}Zr^{++}$ (1 s), $^{49}Ti^{+}$ (10 s) by magnetic peak scan. The typical intensity of the ^{30}Si peak was $\sim 7 \times 10^4$ cps (counts per second). The internal precision of a single analysis (five cycles, 7–8 min in total including presputtering) yielded better than 5% (1SD) at the 5 ppm level.

Ti concentrations were calculated using NIST 610 glass (434 ppm Ti) as a running standard as a widely available zircon standard with certified homogeneous Ti concentration has yet to be developed. In order to assess potential matrix effects between zircon and glass, a relative sensitivity factor (RSF) of $^{49}Ti/^{30}Si$ in the glass standard was compared with a zircon of known Ti concentration in the same analytical session. Synthetic, Ti-doped zircons (800–1500 ppm Ti, synthesized by E.B. Watson) were analyzed by electron microprobe in order to estimate the RSF (Electronic Annex 1). The RSF of $^{49}Ti/^{30}Si$ in zircon was found to be slightly higher than that of the NIST 610 glass. For this reason, we apply a correction factor (1.16) to the RSF of the NIST 610 glass standard measured during each analysis session.

3.3. Analysis of Ti, REE, Y, and Hf

Rare Earth Elements, Y, Hf, and Ti were measured at the same time on selected zircons. The primary beam conditions, spot size, secondary ion optics, and monocollection were the same as when Ti was analyzed alone, and analysis was performed at the same MRP (~4500). However, the field aperture was increased to 5000 μm for better transmission. A 42 V energy offset was applied to the secondary beam in order to minimize molecular interference, and was sufficient to allow resolution of the selected REE peaks from the interfering REE oxides. Analyses consisted of 1 min presputtering followed by seven mass scans of the following isotopes: ^{30}Si (2 s), ^{49}Ti (5 s), ^{89}Y (3 s), ^{91}Zr (1 s), ^{139}La (20 s), ^{140}Ce (5 s), ^{141}Pr (10 s), ^{145}Nd (10 s), ^{147}Sm (10 s), ^{153}Eu (10 s), ^{159}Tb (5 s), ^{160}Gd (5 s), ^{163}Dy (5 s), ^{165}Ho (5 s), ^{166}Er (5 s), ^{169}Tm (5 s), ^{172}Yb (3 s), ^{175}Lu (3 s), ^{178}Hf (3 s), for a total analysis time of 20 min. Data were collected only from the last five scans of each analysis, the first two magnet scans were used as presputtering to eliminate surface contamination. Measured counts for each element were normalized to ^{30}Si, standardized to NIST 610 glass and monitored with zircon standard 91500 (Wiedenbeck et al., 2004). Because of the markedly different REE composition of NIST 610 glass and natural zircons, counting times were adjusted for NIST 610 as follows: ^{30}Si (2 s), ^{49}Ti (5 s), ^{89}Y (3 s), ^{91}Zr (5 s), ^{139}La (3 s), ^{140}Ce (3 s), ^{141}Pr (3 s), ^{145}Nd (10 s), ^{147}Sm (10 s), ^{153}Eu (5 s), ^{159}Tb (3 s), ^{160}Gd (10 s), ^{163}Dy (10 s), ^{165}Ho (3 s), ^{166}Er (5 s), ^{169}Tm (3 s), ^{172}Yb (10 s), ^{175}Lu (3 s), and ^{178}Hf (5 s). Typical count rates (counts per second) in NIST 610 glass are ^{30}Si: 1.8×10^5 cps, ^{140}Ce: 4.5×10^3 cps, ^{178}Hf: 2.8×10^2 cps. Typical count rates in zircon 91500 are ^{30}Si: 8.4×10^4 cps, ^{140}Ce: 1.7×10^1 cps, ^{178}Hf: 3.2×10^3 cps. Because of the matrix difference between glass and zircon, REE and Hf values for standard 91500 were underestimated when standardized to NIST 610 alone. An RSF of 1.25 was applied to each element analyzed to compensate for this matrix effect. This RSF differs from the RSF applied to Ti-only analyses (Section 3.2) because an energy offset was not applied to Ti-only analyses. Comparison of Ti concentrations in zircon KIM-5 between Ti-only analyses without energy offset and multiple element analyses with energy offset give consistent results.

4. RESULTS

4.1. Oxygen isotopes

The oxygen isotope ratios of zircon megacrysts from kimberlites from South Africa and Siberia were reported by Valley et al. (1998). The average $\delta^{18}O$ of these zircons is 5.3‰, in equilibrium with olivine from peridotites (Mattey et al., 1994) and olivine phenocrysts from Hawaii (Eiler et al., 1996). The variability in $\delta^{18}O$ of kimberlite zircons is greater than that found in mantle olivines, and subtle pipe-to-pipe variation in $\delta^{18}O$ was recognized. A brief summary of the $\delta^{18}O$ results from Valley et al. (1998) on zircons measured for Ti and REE concentrations in this study is provided in Sections 4.1.1 and 4.1.2 followed by new $\delta^{18}O$ data from Brazil.

4.1.1. Kaapvaal craton

Zircons from kimberlites of the Kaapvaal craton (Fig. 1) were analyzed for $\delta^{18}O$ by Valley et al. (1998) and a summary of those data are presented in Table 1 and Fig. 5. Individual zircons that were analyzed multiple times (core vs. rim) by laser fluorination were found to be homogeneous in $\delta^{18}O$, and zircons from most individual pipes also have little variability, suggesting that the zircons from each pipe are the products of distinct igneous/metasomatic events. Zircons of different ages from the Jwaneng kimberlite were found to have different $\delta^{18}O$, with Precambrian zircons displaying much more variability and lower values than the Permian group. Despite the overall limited range of $\delta^{18}O$ values in mantle zircons, subtle pipe-to-pipe variability was found to exist among several African kimberlites. Subtle variability between zircon populations from different pipes was interpreted as a reflection of variable incorporation of oxygen from a subducted component of the SCLM.

4.1.2. Siberian craton

Zircons from Siberian kimberlites (Fig. 2) were also analyzed for $\delta^{18}O$ by Valley et al. (1998), and summarized in Table 1 and Fig. 5. The sample set from Siberia consists of previously ion-probed zircons (U–Pb), and fewer zircons from each kimberlite were available for study. Nonetheless, the zircons analyzed from each pipe were found to have very small variability. Overall, the average $\delta^{18}O$ of zircons from Siberian kimberlites (5.2‰) is similar to African zircons (5.3‰), but the differences between different pipes appear to be more distinct. One zircon from the Ukukit Leningrad pipe has an anomalously high $\delta^{18}O$ (7.1‰) and an anomalously old age relative to other zircons from the same district. For these reasons, Valley et al. (1998) interpreted this zircon as crustal, and excluded it from the mantle averages.

Table 1
Summary of $\delta^{18}O$, Ti concentration, and thermometry, by kimberlite pipe

Pipe	$\delta^{18}O$-zircon (‰VSMOW)	Number of Ti analyses	Number of zircons	Ti (ppm)			T (°C)[a]		
				max	min	Avg. 1SD	max	min	Avg. 1SD
Kaapvaal Craton									
Kaalvallei Mine	5.32[c]	5	5	25	17	21 ± 3.3	829	792	811 ± 16
Balmoral Mine	5.45[c]	11	5	13	7.9	11 ± 1.7	762	721	747 ± 14
Kamfersdam Mine	5.18[c]	5	5	15	3.2	9.3 ± 4.9	775	651	725 ± 52
Leicester Mine	5.30[c]	14	7	13	7.8	11 ± 1.5	764	720	751 ± 12
Kimberley Pool	5.35[c]	51	5	21	3.3	5.4 ± 2.2	810	652	683 ± 26
Jwaneng DK2, Precambrian	4.69[b,c]	2	1	35	25	30 ± 7.0	866	830	848 ± 25
Jwaneng DK2, Permian	5.73[c]	2	1	3.7	2.0	2.8 ± 1.2	661	616	638 ± 31
Orapa rutile-bearing suite	5.55[c]	15	14	22	13	16 ± 2.6	814	767	784 ± 15
Orapa chromite-bearing suite	n.a.	9	9	19	10	13 ± 2.9	800	742	766 ± 19
Kaapvaal-Summary	5.32[c]	114	52	35	2.0	13 ± 8.4	866	616	750 ± 63
Siberian Platform									
Orto-Yarga, Anomaly 12/853	4.98[c]	6	2	28	21	25 ± 2.2	840	811	827 ± 10
Chomurdakh, Khaiyrgastakh	4.73[c]	2	1	2.5	2.3	2.4 ± 0	632	626	629 ± 5
Chomurdakh, Anomaly 180/78	5.07[c]	3	2	11	6.8	9.5 ± 3.6	747	709	736 ± 54
Ukukit West, Leningrad	7.09[b,c]	2	1	19	17	18 ± 1.7	800	787	794 ± 9
Ukukit West, Anomaly 134	5.26[c]	2	1	3.4	2.3	2.9 ± 0.8	655	627	641 ± 19
Ukukit West, Anomaly 152	5.02[c]	2	1	9.6	9.2	9.4 ± 0.3	737	734	736 ± 3
Mir	5.53[c]	7	4	10	7	9 ± 1.3	745	715	734 ± 13
Siberia-Summary	5.16[c]	17	8	28	2.3	10 ± 8.1	840	626	717 ± 73
Brazil-Alto Paranaba district									
Ponte Funda	5.20	8	1	17	5	11 ± 5.1	789	688	740 ± 45
São João da Glória	5.33	4	1	19	10	14 ± 4.4	800	737	770 ± 30
Fazen da Inaçao	4.87	2	1	6.4	4.8	5.6 ± 1.1	703	680	691 ± 16
Botafogo	5.28	2	1	20	13	16 ± 4.4	803	767	785 ± 26
Vargem 4B	5.49	6	1	51	34	43 ± 6.6	908	868	887 ± 18
Buriti	5.05	2	1	18	16	17 ± 0.8	793	786	789 ± 5
Tatão	5.28	3	1	36	26	30 ± 5.0	867	832	848 ± 18
Morro do Lobo	5.12	8	1	13	6.2	9.1 ± 2.4	763	702	731 ± 23
Cedro	8.25[b]	4	1	86	34	63 ± 22	974	862	927 ± 47
Japecanga	5.17	13	2	53	9.2	20 ± 12	912	734	795 ± 57
Capão da Erva	5.55	6	1	29	6.5	12 ± 8.6	844	705	744 ± 52
Almas	5.08	3	1	18	13	15 ± 2.3	793	764	778 ± 14
Canas AN32	5.08	0	1	n.a.	n.a.	n.a.	n.a.	n.a.	n.a.
Canastrel	5.48	0	1	n.a.	n.a.	n.a.	n.a.	n.a.	n.a.
Descida para Vargem	5.51	0	1	n.a.	n.a.	n.a.	n.a	n.a.	n.a
Galeria	5.25	0	1	n.a.	n.a.	n.a.	n.a.	n.a.	n.a.
Morunga	5.28	0	1	n.a.	n.a.	n.a.	n.a.	n.a.	n.a.
Poço Verde	5.82	0	1	n.a.	n.a.	n.a.	n.a.	n.a.	n.a.
Tamborete	5.60	0	1	n.a.	n.a.	n.a.	n.a.	n.a.	n.a.
Vargem 1, Poço 9	5.31	0	1	n.a.	n.a.	n.a.	n.a.	n.a.	n.a.
Velosa	7.53[b]	0	1	n.a.	n.a.	n.a.	n.a.	n.a.	n.a.
Represinha	7.31[b]	0	1	n.a.	n.a.	n.a.	n.a.	n.a.	n.a.
Alto Paranaibo-Summary	5.30 ± 0.23	61	23	86	4.8	18 ± 11	974	680	778 ± 68
Brazil-Juina district									
Acuri	5.02	2	1	6.8	6.8	6.8 ± 0.0	708	708	708 ± 1
Mutum	4.80	2	1	8.2	7.3	7.8 ± 0.6	724	715	719 ± 7
Duas Barras	4.92	2	1	6.5	6.3	6.4 ± 0.1	704	702	703 ± 2
Junía-Summary	4.91 ± 0.11	6	3	8.2	6.3	7.0 ± 0.7	724	702	710 ± 8
Brazil-Summary	5.11 ± 0.28	67	26	86	4.8	12 ± 7.5	974	680	744 ± 48
Midwest United States									
Six-Pak, Kenosha, Wisconsin	5.09 ± 0.12	3	1	2.2	1.3	1.8 ± 0.5	623	589	608 ± 18
Site 73, Hermansville, Mich.	5.47	2	1	9	6.7	7.9 ± 1.6	732	707	719 ± 18
U.S.-Summary	5.28 ± 0.27	5	2	9	1.3	4.8 ± 4.3	732	589	664 ± 78

SD, Standard deviation, n.a., not analyzed.
[a] Watson and Harrison (2005).
[b] Anomalous $\delta^{18}O$, excluded from mantle averages.
[c] Data from Valley et al. (1998).

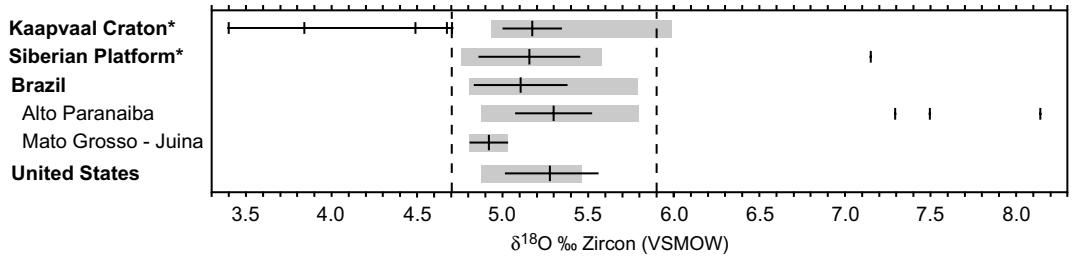

Fig. 5. Values of $\delta^{18}O$ for mantle zircon megacrysts from kimberlite. The craton average and 1SD are shown in black with the total range in gray. Dashed lines show the 2SD range of values around the average kimberlite zircon $\delta^{18}O$ from Valley et al. (1998). Samples with anomalously high or low $\delta^{18}O$ are suspected crustal xenocrysts and are shown as individual data points. *Data for Africa and Siberia are from Valley et al. (1998).

4.1.3. Brazil

Oxygen isotopes were measured by laser fluorination in zircons from 25 pipes in two kimberlite districts of Brazil (Fig. 3). Values of $\delta^{18}O$ range from 4.80‰ to 8.25‰ (Table 1, Fig. 5). Zircons from the Juina district have lower average $\delta^{18}O$ (4.91 ± 0.11‰ 1SD, $n = 3$) whereas zircons from the kimberlites of the Alto Paranaiba district have higher average $\delta^{18}O$ (5.30 ± 0.23‰, $n = 19$); three zircons from three kimberlites in the Alto Paranaiba district (Cedro, Velosa, and Represinha) yielded anomalously high $\delta^{18}O$ of 7.31–8.25‰. Although these zircons may record local $\delta^{18}O$ enrichment within unmixed mantle domains, they may also be the products of crustal contamination, similar to one Ukukit Leningrad zircon. Because their oxygen isotopic composition is so markedly different from the bulk of the zircons from this district (and, where available, their trace element composition differs from other mantle zircons), these high $\delta^{18}O$ zircons will be considered separately in the discussion, and are not included in the district average. The average oxygen isotopic composition of mantle zircons from the Alto Paranaiba and Juina kimberlite provinces of Brazil is 5.11 ± 0.28‰, and is consistent with the craton-wide averages for Siberia (5.16 ± 0.30‰) and the Kaapvaal craton (5.32 ± 0.17‰) from Valley et al. (1998).

4.1.4. Midwest United States

A number of (sub-economic) diamondiferous diatremes have been discovered in the Midwest United States (principally in the Upper Peninsula of Michigan) since the early 1970's (Cannon and Mudrey, 1981; McGee and Hearn, 1983; Carlson and Floodstrand, 1994). Zircon megacrysts from mineral concentrates of two diamond prospects in Michigan and Wisconsin were analyzed for $\delta^{18}O$, and are presented in Table 1 and Fig. 5. One fragment of a zircon from the Site 73 kimberlite, Hermansville, Michigan (Carlson and Floodstrand, 1994) has $\delta^{18}O = 5.47$‰. Fragments of six zircon megacrysts from the Six-Pak lamprophyre diatreme, Kenosha, Wisconsin (Carlson and Adams, 1998) were analyzed and have $\delta^{18}O = 5.09 \pm 0.12$‰.

4.2. Titanium

Zircon megacrysts from kimberlites on four cratons were analyzed for their Ti content by ion microprobe. Polished 1–2 mm zircons or fragments of larger megacrysts were imaged by CL, revealing the characteristic fine-scale oscillatory zoning common in this type of zircon (Fig. 4). At least two ion microprobe analyses were performed on each zircon fragment, and analysis location was guided by CL in order to analyze different growth zones and characterize possible intracrystalline zoning in Ti. In most cases, the one set of parallel growth zones visible in the megacryst fragment did not allow the distinction between the early and late growth zones to be made, but analyses were made across the zonation to maximize the possibility of observing any heterogeneity (Figs. 4c–e). Two zircons from kimberlites in the Alto Paranaiba province of Brazil (São João da Glória and Ponte Funda) show evidence of secondary recrystallization in CL (e.g., Fig. 4f), coupled with a decrease in Ti concentration in the recrystallized zones (cf. Holden et al., 2005). The Ti concentration of each analysis is plotted in Fig. 6 and reported in Electronic annex EA-2. Kimberlite pipe averages are reported in Table 1 and plotted in Fig. 7 in conjunction with oxygen isotopic composition.

4.2.1. Kaapvaal craton

The titanium content of zircon megacrysts from the Kaapvaal Craton ranges from 2.0 to 35 ppm (Figs. 6 and 7a). Both the minimum and maximum values come from the Permian and Precambrian zircons of the Jwaneng DK2 kimberlite (Botswana), respectively. Zircons from the Jwaneng DK2 kimberlite have anomalously high (Permian samples) and low (Precambrian samples) $\delta^{18}O$ (Valley et al., 1998), and are likely crustal in origin. The craton-wide average (excluding Jwaneng) is 13 ± 8.4 ppm (1SD), and the range is 3.3–25 ppm. Variability in Ti is evident within single zircons, between zircons in a single pipe, and between pipes throughout the region.

Zircons from the Balmoral ($n = 4$), Leicester ($n = 7$) and Kaalvallei ($n = 5$) kimberlites display the least variability in Ti. Fragments of different zircons from the Leicester kimberlite are homogeneous in Ti within analytical uncertainty. Zircons from the adjacent Balmoral and Leicester mines have indistinguishable average Ti content, 11 ± 1.7 ppm and 11 ± 1.5 ppm, respectively. Zircons from Kaalvallei contain significantly more Ti (21 ± 3.3 ppm) with slightly more intercrystalline variability.

Five megacrysts, each measuring ~1 cm in diameter, from the Kimberley Pool of kimberlites were analyzed for Ti. Four of these megacrysts (KIM-1, KIM-3, KIM-4, and KIM-5) have similar Ti concentrations with an average

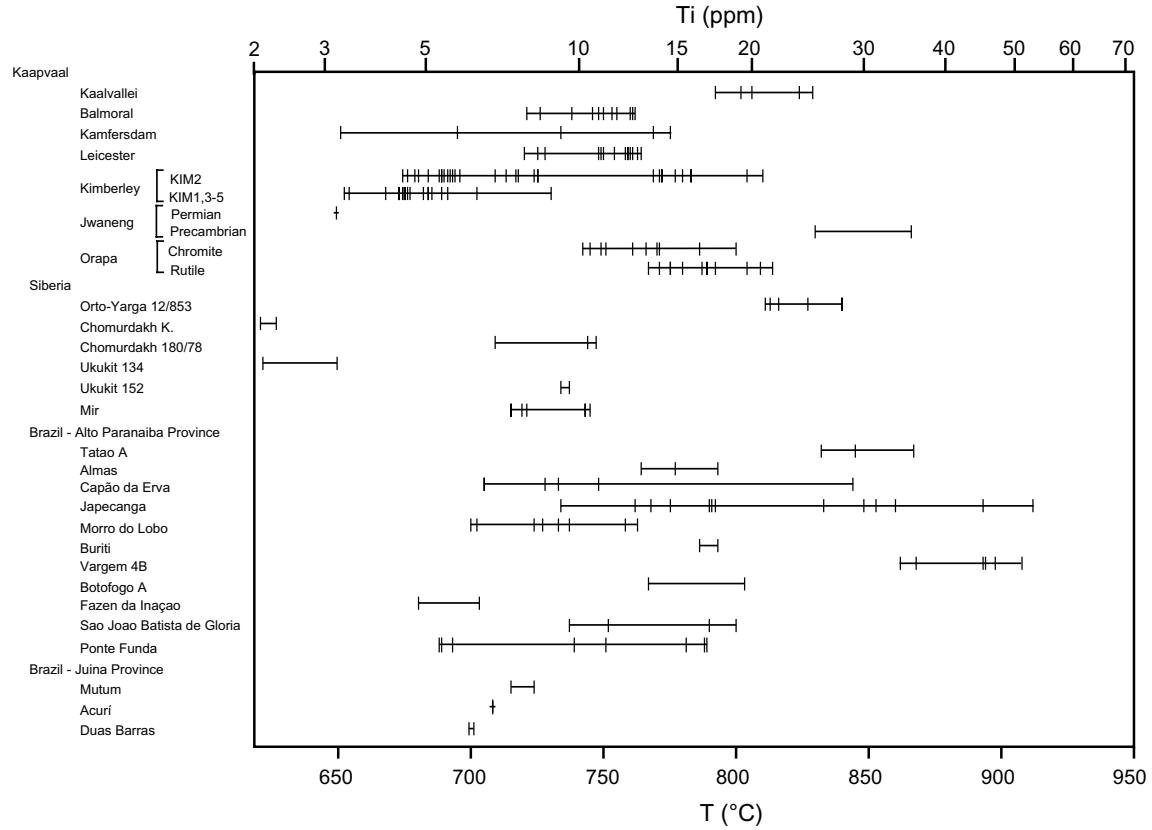

Fig. 6. Ti concentration and estimated temperature (Watson and Harrison, 2005) for kimberlite zircons. Each data point corresponds to one analysis.

of 5.4 ± 2.2 ppm. Three of the megacrysts were analyzed for Ti two times each (KIM-1, KIM-3, KIM-4) and have limited variability in their Ti content, similar to megacrysts from Balmoral, Leicester and Kaalvallei. The oxygen isotope standard KIM-5 (5.1 ± 1.2 ppm Ti) has been analyzed more exhaustively (14 analyses on eight fragments) and is significantly more variable in its Ti content. This greater variability is largely explained by two analyses (8.8 and 6.3 ppm) and if these are excluded, variability becomes comparable to KIM-1, KIM-3, and KIM-4. The two high Ti analyses are from different ~300 μm fragments of KIM-5, and additional analyses on these fragments yield less anomalous Ti concentrations of 4.4–5.0 ppm, suggesting that KIM-5 contains small (≪300 μm) regions of Ti enrichment. No spikes in Ti concentration were observed during analysis, suggesting that Ti enrichment is not the result of the analysis of small inclusions. The remaining zircon analyzed from the Kimberley Pool (KIM-2) displays similar, patchy zones of enrichment in Ti, but of greater magnitude. The ~1 mm fragment of zircon KIM-2 initially analyzed ranges from 4.4 to 15 ppm Ti (Fig. 4a) with Ti increasing across CL zoning but with no clear change in CL intensity. In order to further explore this heterogeneity, additional analyses were made on a polished section of the full megacryst (10 × 12 mm). Regions of KIM-2 range up to 21 ppm Ti with an average of 9.2 ± 4.9 ppm over 31 analyses. No clear correspondence was found between CL zoning and regions of higher Ti. The Kamfersdam mine (also in Kimberley, but processed separately than the KIM samples) also has significant variability in Ti between the five zircons analyzed from a single pipe (9.3 ± 4.9 ppm, 1SD). However, only one analysis was done on each zircon (during REE analysis), and intracrystalline variability is unconstrained (Fig. 4b).

Zircons from two different paragenetic suites were analyzed from the Orapa (Botswana) kimberlite. Zircon megacrysts with chromite inclusions contain 13 ± 2.9 ppm Ti. Zircons found in rutile nodules (Schulze, 1990) contain only slightly more Ti (16 ± 2.6 ppm).

4.2.2. Siberian craton

Zircon megacrysts from seven Siberian kimberlites contain 10 ± 8.1 ppm Ti (2.3–28 ppm) and display similar variability to samples from the Kaapvaal Craton. Zircons from the Mir kimberlite field (9 ± 1.3 ppm Ti,) and the Orto-Yarga kimberlite (25 ± 2.2 ppm) are the least variable from the Siberian Craton, and have similar variability in Ti to zircons from the Leicester and Balmoral kimberlites of the Kaapvaal Craton. Zircons from the Orto-Yarga kimberlite are the most Ti-rich from Siberia. Zircons from different pipes of the Ukukit and Chomurdakh fields display a wide range in Ti content. In the Chomurdakh field, a zircon from one pipe (Khaiyrgastakh) contains anomalously low Ti (2.4 ± 0.2 ppm), whereas two zircons from another pipe (Anomaly 180/78, Fig. 4d) in the same field have greater and more variable Ti (9.5 ± 3.6 ppm). The low Ti content

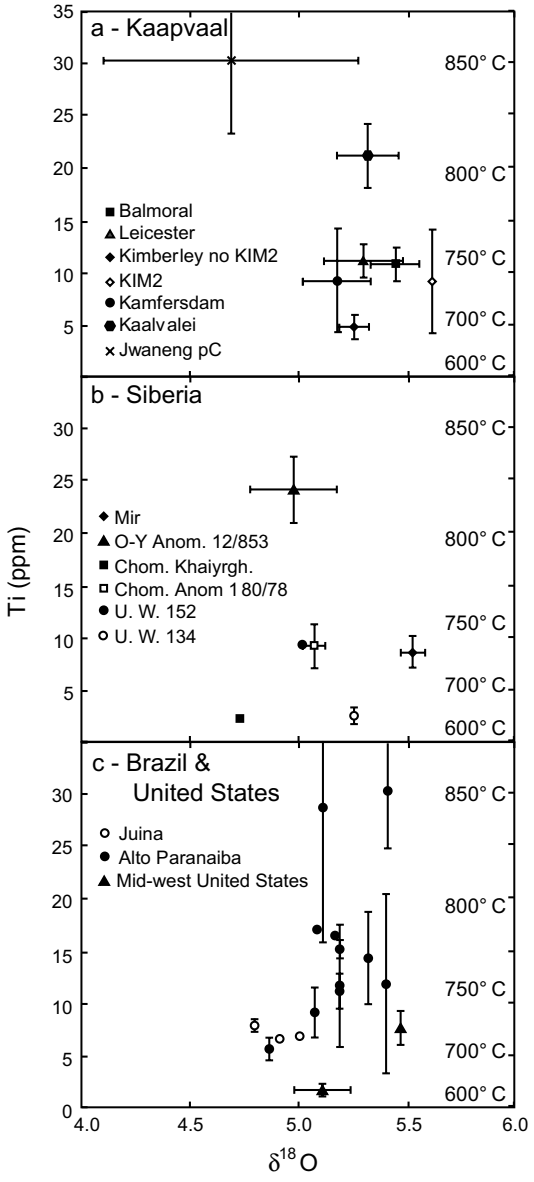

Fig. 7. Average Ti concentration and $\delta^{18}O$ in zircon for kimberlites from (a) Africa, (b) Siberia, and (c) Brazil and U.S. Kimberlite averages are plotted with 1SD error bars where more than one analysis was made.

for the Khaiyrgastakh zircon corresponds to anomalously low $\delta^{18}O$. Similarly, the high Ti content (18 ± 1.7 ppm) of the Leningrad kimberlite zircon corresponds with high $\delta^{18}O$ (7.09‰), which is hypothesized as crustal in origin.

4.2.3. Brazil

Titanium in zircons sampled from 13 Brazilian kimberlites averages 12 ± 7.5 ppm; zircon from the Cedro pipe contains unusually high Ti (up to 86 ppm). This high Ti content is coupled with a higher $\delta^{18}O$ value (8.25‰) in a manner similar to the Leningrad kimberlite in Siberia. Unfortunately, no material from the Velosa and Represinha high $\delta^{18}O$ zircons was left after laser fluorination for trace element analysis. Zircons from the three sampled pipes of the Juina province (Duas Barras, Acuri and Mutum) have lower Ti (7.0 ± 0.7 ppm) than zircon from 10 sampled kimberlites of the Alto Paranaiba district (18 ± 11 ppm). In all but one case (Japecanga) only one zircon was analyzed for each pipe, and so within-pipe variability is unconstrained. The two zircons analyzed from the Japecanga pipe display some variability (12 vs. 23 ppm). Zircons from the Alto Paranaiba province have greater within-crystal heterogeneity, coupled with more complicated zoning patterns in CL, than the other samples in this study. Two zircons show evidence of recrystallization in the form of diffuse blue CL zones that partially to completely obscure primary yellow oscillatory zoning (Fig. 4f). This recrystallization may be a result of interactions with late melts or metasomatizing fluids in the mantle, or possibly during entrainment by the kimberlite. In both cases (São João da Glória and Ponte Funda) the recrystallized zones contain 5–10 ppm less Ti than do regions with clear primary zoning.

4.2.4. Midwest United States

Zircons from two kimberlites in the Midwest United States contain relatively little Ti (4.8 ± 4.3) and are markedly different from each other. One zircon from the Site 73 kimberlite (Michigan) contains 7.9 ± 1.6 ppm Ti. Zircons from the Six-Pak site (Wisconsin) are the most Ti-poor of this study, containing 1.8 ± 0.5 ppm Ti.

4.3. Rare earth elements

A subset of zircons was selected for REE analysis by ion microprobe in a separate analytical session. In addition to the REE, Ti, Hf, and Y were also analyzed. Results are tabulated in Electronic annex EA-3, and presented in Fig. 8. The REE data collected from most of these zircons are broadly consistent with published REE data from zircon megacrysts (Belousova et al., 1998; Hoskin and Ireland, 2000; Belousova et al., 2002). The average compositions of zircons from the four continents display the classic chondrite-normalized REE patterns of kimberlite zircon with low total REE abundance, no Eu anomaly, and flat heavy and middle REE patterns (Fig. 8a). The variability in the average zircon REE patterns between cratons is similar to the range in any given craton (e.g., Kaapvaal, Fig. 8a), confirming that most zircons from kimberlite are characterized by this distinctive pattern. Approximately 20% of the zircons analyzed for REE in this study (including zircons from each craton except N. America, where only one zircon was analyzed) have elevated REE compared to literature values of zircons from kimberlite (Belousova et al., 1998, 2002). These zircons have a similar chondrite-normalized REE pattern to the other zircons, but with REE contents of 100 to ~650 ppm (as opposed to ⩽60 ppm for most kimberlite zircons. These REE patterns are similar to those of zircons from carbonatites, and are not uncommon among kimberlite zircons as well (Belousova et al., 2002) (Fig. 8).

4.3.1. Kaapvaal craton

There is no broad correlation between Ti concentration, REE concentration or chondrite-normalized pattern slope

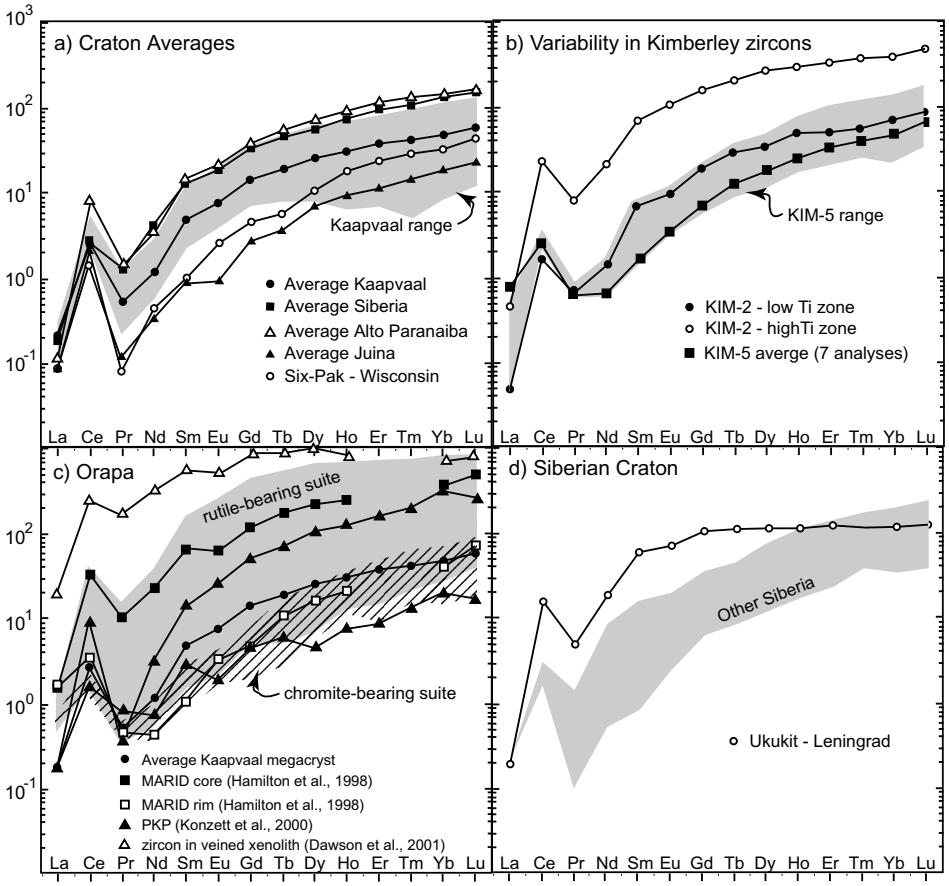

Fig. 8. Chondrite-normalized REE diagrams for selected zircons. (a) Average composition of zircons from kimberlite from five cratons on four continents. The range of compositions from the Kaapvaal Craton is shown in gray and is similar to the range of averages. (b) Zircons KIM-2 and KIM-5. Ti-rich zones of zircon KIM-2 from the Kimberley Pool, Kaapvaal Craton are elevated in REE relative to the Ti-poor zones and zircon KIM-5. (c) Zircons from the two different suites of megacrysts from the Orapa kimberlite (Kaapvaal Craton) have similar Ti compositions, but different REE systematics. The rutile nodule suite overlaps both typical megacryst REE values and those of zircons from metasomatic xenoliths. (d) A zircon from the Ukukit Leningrad pipe has a crustal $\delta^{18}O$ (7.09‰) but has a REE pattern similar but more elevated than most mantle zircons. The range of compositions of other Siberian Craton zircons is shown in gray.

and $\delta^{18}O$ in zircons from the Kaapvaal Craton. However, in certain specific cases, Ti and REE content are correlated on the intracrystalline scale. Low Ti zones found in the variable Ti-content zircon KIM-2 of the Kimberley Pool (Kaapvaal Craton) have similar Ti and REE to zircon KIM-5 (Fig. 8b). However, the high Ti zones in KIM-2 are significantly enriched in REE with a carbonatite-like pattern.

Zircons from the Orapa, Botswana kimberlite have the highest concentrations of REE of all those measured in this study (Fig. 8c). Zircons from the chromite-bearing suite of megacrysts have an average REE composition quite similar to the Kaapvaal average, and are variable on the same scale as most other kimberlites. Zircons associated with rutile-dominated nodules, however, are much more widely variable (Fig. 8c). Zircons from this suite range from typical kimberlite patterns that overlap with the chromite suite at lower concentrations than the craton average, to the most extremely elevated carbonatite-like pattern with $\Sigma REE = 650$ ppm. The more elevated REE patterns from the Orapa-rutile suite are higher than the elevated REE values found in the cores of MARID zircons (Hamilton et al., 1998) and PKP zircon (Konzett et al., 2000) and approach the values found in a zircon-bearing veined harzburgite xenolith (Dawson et al., 2001; Fig. 8c). Although a MARID zircon rim and a PKP zircon have REE patterns that overlap with typical kimberlite patterns, the Orapa rutile suite is the first group of zircons with an origin in the mantle that spans the range of megacryst and metasomatic zircon REE.

4.3.2. Siberia

From the Siberian craton, one zircon from kimberlite Ukukit Leningrad has a carbonatite REE pattern (possibly with some MREE enrichment as well) distinct from the other Siberian zircons in this study (Fig. 8d). The Ukukit Leningrad zircon is also anomalous in its oxygen isotope ratio (7.09‰).

4.3.3. Brazil

Both the REE and Ti content of the Juina province zircons is markedly lower than zircons from the Alto

Paranaiba province (Fig. 8a). One zircon from the São João da Glória kimberlite (Alto Paranaiba, Brazil) shows evidence of recrystallization in CL (Fig. 4f). The core region (Ti ~20 ppm, ΣREE ~124 ppm) is also elevated in the REE relative to the recrystallized rims (~10 ppm Ti, ΣREE ~44 ppm, Table EA-3). Unlike the Siberian zircon with an elevated REE signature (Ukukit Leningrad), these zircons from the Alto Paranaiba district of Brazil do not have elevated $\delta^{18}O$.

4.4. Ti-thermometry

The Ti content of zircon has been calibrated as a geothermometer against a suite of experimentally synthesized and natural samples. (Watson and Harrison, 2005; Watson et al., 2006). The published calibration of Watson et al. (2006) was applied to the Ti concentrations measured in these zircons from kimberlite. As noted, the Ti concentration of these zircons is quite low, and they result in calculated temperatures on the order of 750 °C. This result is surprisingly low for mantle phases, and raises questions of the applicability of this thermometer to these zircons, or even to the calibration itself.

Variability in Ti in kimberlite zircons is clearly resolvable on a variety of scales (Section 4.2). However, the extreme temperature sensitivity of the Ti in zircon thermometer has the effect of smoothing this variability. If the concentration of Ti in the zircons in this study is purely a function of formation temperature, then a typically observed variability in Ti of 20% at the 10 ppm level (i.e. 10 ± 2 ppm) results in a change in estimated temperatures of only 17 °C. It is unclear if a temperature difference such as this is real given the caveats presented in this section. Even if such variability is a product of subtle temperature differences, it is unlikely that such differences are geologically meaningful.

4.4.1. Kaapvaal craton

The Ti content of zircons from the Kaapvaal craton yields a temperature range from 616 to 866 °C, constrained by Ti values from the Jwaneng DK2 kimberlite. The craton average is 750 ± 63 °C. Other than Jwaneng, the hottest temperatures recorded are from Kaalvallei (811 ± 16 °C). Zircons from the geographically associated Leicester (751 ± 12 °C) and Balmoral (747 ± 14 °C) mines formed at identical temperatures, within error of more variable temperatures from Kamfersdam (725 ± 52 °C), and ~70° hotter than zircons from Kimberley (683 ± 31 °C). Temperatures recorded by KIM-2 range from 676 °C to 810 °C. Zircons from the Orapa rutile nodule suite record 784 ± 15 °C and those from the chromite-bearing suite record essentially the same temperatures (766 ± 19 °C).

4.4.2. Siberian craton

Kimberlite zircons from the Siberian Platform record a similar average temperature to the Kaapvaal samples of 717 ± 73 °C. Samples from two pipes in two different districts yielded significantly greater Ti (and temperature) than other Siberian samples. Two zircons from the Orto-Yarga Anomaly 12/853 pipe yield temperatures of 820–834 °C and one high-$\delta^{18}O$ zircon from the Ukukit Leningrad pipe contains Ti consistent with formation at 794 °C. All zircons from the Orto-Yarga Anomaly 12/853 pipe have mantle-like $\delta^{18}O$, suggesting real variability in the temperatures of formation for mantle zircon. Zircons from the Chomurdakh Khaiyrgastakh kimberlite record lower temperatures of formation (626 °C) than zircons from the Chomurdakh Anomaly 180/78 pipe from the same field (728–744°). This low temperature for the Chomurdakh Khaiyrgastakh kimberlite corresponds to similarly low $\delta^{18}O$ (Fig. 7b).

4.4.3. Brazil

The average temperature recorded by zircons from the Alto Paranaiba kimberlite province (778 ± 68 °C) is similar to those of the majority of samples from Africa and Siberia. One zircon from the Cedro kimberlite records high and variable temperature (862–972 °C), but has $\delta^{18}O$ (8.25‰) outside of the typical mantle range. A zircon from the Vargem 4B pipe is a fragment that shows oscillatory concentric zoning in CL. Titanium decreases core to rim, from 51 ppm to 36 ppm yielding a narrow temperature range of 908–826 °C, but significantly higher than other zircons in this study with $\delta^{18}O$ of 5.75‰. Two zircons from the Japecanga kimberlite record significantly different temperatures. One zircon shows oscillatory zoning in CL and records a range of temperatures (775–912 °C) while the other zircon, which is clearer in transmitted light and has low, unzoned CL, records lower and more homogenous temperatures (734–768 °C). Zircons from the three pipes of the Juina province record lower and less variable temperatures than the Alto Paranaiba district zircons (710 ± 8 °C, three zircons, six analyses).

4.4.4. Midwest United States

The Ti concentrations of zircons from the Site 73 kimberlite (Michigan) yields a temperature of 719 ± 18 °C. The unusually low-Ti concentrations of zircons from the Six-Pak site (Wisconsin) yield a temperature of 608 ± 18 °C.

5. DISCUSSION

A hallmark of zircons from kimberlite appears to be relatively homogeneous oxygen isotope ratios, REE systematics and Ti concentrations on a global scale. Subtle differences in these and other geochemical tracers may yield important insight into the nature of the mantle systematics beneath ancient cratons, but zircons from kimberlites from four continents appear to have more similarities than differences. Given their global nature, these similarities are likely due to the mechanism of formation of zircons sampled by kimberlite. Perhaps the most striking of these similarities is the low and relatively homogeneous Ti concentration that yields a surprisingly low temperature of formation based on the current formulation of the Watson et al. (2006) thermometer. Similarly, surprisingly low temperatures of formation have been reported for crustal igneous rocks as well (Fu et al., 2005).

5.1. Oxygen isotopes

Zircon megacrysts from kimberlites from the Kaapvaal and Siberian cratons have been shown to record a limited range of $\delta^{18}O$ consistent with magmatic formation from a relatively homogeneous mantle reservoir as opposed to the more variable $\delta^{18}O$ found xenoliths of metamorphic origin (e.g., Deines et al., 1991). New oxygen data from mantle zircons from Brazil and the United States are closely similar to the $\delta^{18}O$ of the other cratons, further supporting this hypothesis. In addition, zircons from the Juina province have $\delta^{18}O$ distinctly lower than zircons from the Alto Paranaiba province reflecting distinct reservoirs in the mantle, or perhaps varying degrees of interaction with isotopically heterogeneous subcontinental lithospheric mantle (SCLM). This difference in $\delta^{18}O$ may reflect the contrasting geology of the two kimberlite districts: Juina is located within the Amazonas craton, while Alto Paranaiba is located at the margin of the São Francisco craton. Perhaps kimberlite emplacement within the mobile belts at the margins of cratons allows for sampling of more heterogeneous material by the zircon precursor melts.

5.2. Ti-thermometry of zircon

If the low temperatures for zircon formation in this study estimated after Watson et al. (2006) are correct, they suggest crystallization at relatively shallow depths in the lithospheric mantle. The average temperature for kimberlite zircon projected on the 40 mW/m^2 geotherm of Pollack and Chapman (1977), that is commonly applied in studies of south African kimberlites, generates pressures of formation of ~3 GPa (Fig. 9). These conditions of formation are at lower pressures than the field of diamond stability. Low crystallization temperatures for zircons in this study would have dramatic implications for the timing of zircon formation relative to kimberlite eruption. Davis et al. (1980) suggested that mantle zircons record the age of kimberlite eruption because of their formation at mantle temperatures above the U–Pb closure temperature in zircon. However, the low temperatures of crystallization from Ti-thermometry are not sufficient to reset age by diffusion of Pb, and thus suggest that U–Pb ages in mantle zircons date crystallization, and are not cooling ages. Is this surprisingly low temperature for zircons from kimberlite a product of nature or of the new Ti in zircon thermometer?

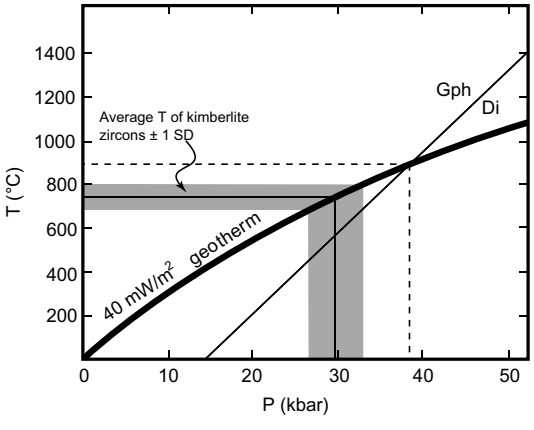

Fig. 9. Average zircon temperatures of formation projected on a cratonic geotherm. Without a pressure or activity correction, the low temperatures of formation yielded by the Ti in zircon thermometer imply shallow depths of formation outside the diamond field of stability.

No direct substitution mechanism is proposed in the calibration of the Ti in zircon thermometer, but the equilibrium for this thermometer must be either:

$$TiO_2 + ZrSiO_4 = TiSiO_4 + ZrO_2 \quad (1)$$

$$\text{rutile} + \text{zircon} = \text{Ti}^{\text{VI}}\text{-zircon} + \text{baddeleyite}$$

or

$$TiO_2 + ZrSiO_4 = ZrTiO_4 + SiO_2 \quad (2)$$

$$\text{rutile} + \text{zircon} = \text{Ti}^{\text{IV}}\text{-zircon} + \text{quartz/coesite}$$

depending upon the coordination of Ti within the zircon structure. Harrison et al. (2005) have suggested that equilibrium (2) is strongly favored based on modeling that employs density functional theory. The principal caveat that Watson et al. (2006) stress in the application of this thermometer is that zircon should have formed in the presence of rutile such that the activity of TiO_2 in the system is unity.

5.2.1. TiO_2 activity

The paragenesis of zircon megacrysts in kimberlite is not well constrained; if the activity of TiO_2 is less than unity, then the thermometer must be strictly regarded as yielding minimum temperatures assuming saturation with respect to all other components. However, megacrysts from most pipes are commonly associated with a Ti-rich phase (rutile or ilmenite), and approximate TiO_2 saturation seems likely. In order to estimate the effect of TiO_2 saturation on the Ti contents of zircons from kimberlite, Ti analyses were made from two distinct suites of zircons from the Orapa kimberlite. One suite of zircons was separated from rutile ± ilmenite ± clinopyroxene nodules (Schulze, 1990). The second suite of zircons are associated with chromite, but not with any titanian phase. Zircons from the rutile-bearing suite average 3 ppm higher in Ti (16 ± 3 ppm, 1SD) than do those from the chromite-bearing, rutile-free suite (13 ± 3 ppm, 1SD), but are not statistically different at the 95% confidence interval.

Because of the widespread occurrence of titanian phases associated with zircons from kimberlite and the similarity in Ti contents of the two Orapa zircon suites, reduced TiO_2 activity does not seem to be a major factor in kimberlite zircons. In any case, reduction of TiO_2 activity to 0.5 will only raise calculated temperatures by 30–60 °C, still resulting in low temperature estimates.

5.2.2. SiO_2 activity

Of equal importance to rutile saturation, but commonly not considered, is the activity of SiO_2. Assuming that the substitution of Ti in zircon is by equilibrium (2). The equilibrium constant for equilibrium (2) is:

$$K_{eq} = \frac{(a_{ZrTiO_4})(a_{SiO_2})}{(a_{TiO_2})(a_{ZrSiO_4})} \quad (3)$$

The presence of SiO_2 is equally important to the equilibrium assemblage as TiO_2. The activity of SiO_2 affects the concentration of Ti in zircon in the opposite sense of TiO_2 activity, but with an equal magnitude. Thus, following the reasoning of Watson and Harrison (2005) reduction of SiO_2 activity to 0.5, should correspond to an increase in the concentration of Ti in zircon by ~5 ppm in the range of concentrations found in most kimberlite zircons. This has recently been confirmed experimentally by Ferry and Watson (2006).

Textural features of many kimberlite zircons offer some constraints to silica activity and the paragenesis of these zircons. Many zircon megacrysts show signs of resorption and are encrusted with ZrO_2 (Kresten et al., 1975) indicative of a desilication reaction with the host kimberlite. This argues against kimberlite as a parent magma of the zircon, and suggests that the zircon formed in a more silica-saturated or lower-T environment than the kimberlite that later entrained it. If the zircons formed within eclogite domains, they may have formed in the presence of quartz, and could have $a_{SiO_2} = 1$. Zircons formed in metasomatic veins or as phenocrysts from a mantle melt have an unconstrained silica activity, but one that is likely less than unity. This effect, taken alone, would require temperature estimates made using Ti in zircon thermometry on mantle zircons to be considered maxima, considering the limited effect of reduced TiO_2 activity. Because of the likely presence of reduced silica activity, another factor other than TiO_2 activity must be invoked to explain the low temperatures.

5.2.3. Pressure effect

Watson et al. (2006) suggest that pressure is not a factor in the use of this thermometer. For most crustal zircons, this may be a valid assumption. However, the calibration experiments for the thermometer were conducted at 1–2 GPa, below the pressures expected for mantle megacryst formation. Given the difference in ionic radii between Ti and Si, one would expect equilibrium (2) to have $\Delta V \neq 0$. If the molar volume of zircon-structured $ZrTiO_4$ is estimated on the basis of other zircon structured phases with tetrahedral substitution (e.g., $ZrGeO_4$) and ionic radii (e.g., Shannon and Prewitt, 1969) the ΔV of equilibrium (2) is estimated to be positive, requiring that with increasing pressure, less Ti can substitute into zircon (Electronic Appendix EA-4). For this reason, without a pressure correction (if activities for TiO_2 and SiO_2 are unity), this thermometer will record minimum temperatures for high-pressure zircons. Any estimation of the magnitude of the pressure correction is difficult to quantify given the extreme dilution of the Ti-zircon and lack of data on the entropy, compressibility and thermal expansion of this phase. Further experiments are required to fully quantify the effect of pressure on the Ti-in-zircon thermometer, especially in further application to mantle and lower crustal rocks.

5.2.4. Constraints on paragenesis

Despite uncertainties in the calibration, the homogeneous nature of Ti in zircons from kimberlite is striking. If the Ti substitution is primarily a function of temperature, the limited range in Ti suggests that zircons in kimberlite form in similar temperature environments. Most individual crystals show no consistent zonation in Ti, and those that do (e.g., Vargem 4B) display Ti variation consistent with less than 100 °C temperature change and are restricted to one locality. With few exceptions, kimberlite zircons appear to grow to a large (mm to cm-scale) size in environments characterized by constant temperatures. This is consistent with formation as a phenocryst phase in a mantle melt or as a vein mineral in the lithosphere, but not consistent with growth as a phenocryst in the rapidly ascending kimberlite magma. Subtle pipe-to-pipe variability is evident in the Ti chemistry of kimberlite zircons as it is in the oxygen isotope chemistry. This may be a reflection of either small temperature or pressure differences or variations in TiO_2 and SiO_2 activity.

Of the 88 zircons in this study, all but eight zircons from five localities have remarkably consistent Ti and O geochemistry ($\delta^{18}O = 4.73–5.82$, Ti < 53 ppm). Zircons from five localities (Jwaneng, Ukukit Leningrad, Cedro, Velosa, and Represinha) have anomalously high or low $\delta^{18}O$. These differences may reflect mantle-source regions that contain a greater crustal (eclogitic) component. Alternatively, Ti, REE and age data (when available) are also anomalous for these samples, and support the hypothesis that these zircons may be crustal in origin, and should not be grouped with zircon formed in the mantle. Zircons from Jwaneng and Ukukit Leningrad have ages that differ greatly from kimberlite emplacement, and also have elevated Ti relative to zircon from neighboring kimberlite. One zircon from the Cedro kimberlite also has anomalously high Ti. A mantle origin for these zircons would be intriguing, and may be worthy of further study. However, given the remarkable homogeneity in oxygen isotopic and Ti temperatures of the majority of zircons from this study, these eight zircons with $\delta^{18}O$ outside the 4.73–5.82‰ range are hypothesized as having a different history.

5.3. Rare earth elements

5.3.1. Correlation with Ti

Similar to Ti, the REE content of mantle zircons is low and quite similar between the four continents sampled. As expected, REE and Ti contents are not correlated in most cases, suggesting that the incorporation of these trace elements into zircon are independent from one another. However, there are a few cases in which Ti and REE are correlated at both the intracrystalline and intercrystalline scales. Zircon from the S. J. Gloria kimberlite (Alto Paranaiba, Brazil) has a yellow oscillatory-zoned core in CL with diffuse blue CL zones of recrystallization at its margin (Fig. 4f). Analyses from the core have elevated Ti (19 ppm) and REE (124 ppm) compared to the recrystallized rims (10 ppm Ti, 44 ppm REE). This can be explained geologically as recrystallization of zircon at lower temperature, pressure, TiO_2 activity or elevated SiO_2 activity coupled with a less REE-rich fluid phase.

Five zircon megacrysts from the Kamfersdam kimberlite in Kimberley form three distinct groups in terms of their REE and Ti systematics (Table EA-3). Two zircons have low Ti (4–7 ppm) and intermediate REE (54–59 ppm).

Two zircons have high Ti (11–17 ppm) and REE (155–167 ppm). A final zircon has high Ti (16 ppm) and very low REE (17 ppm). Only one analysis was made of each of these zircons, and intracrystalline zoning may also be present. However, an alternative explanation is that the zircons from the Kamfersdam kimberlite formed in a more variable P, T, X environment than most other kimberlites. This may be supported by the MARID-like intergrowths commonly found in Kamfersdam zircons (Dawson and Smith, 1977; Kinny and Dawson, 1992). From the Kimberley Pool, zircon KIM-2 is heterogeneous in both Ti and REE. Most analyses of this crystal are similar to other megacrysts from the Kimberley Pool, however, some analyses have elevated Ti (15–20 ppm vs. 6 ppm) correlated with elevated REE (277 ppm vs. 40 ppm). In this case high Ti zones are not correlated with CL zoning (as in the case of the zircon from the S.J. Gloria kimberlite) and cannot be explained as changes in the temperature and fluid composition during crystal growth. These elevated Ti and REE zones are also likely not the result of analysis of sub-microscopic Ti and REE rich phases, as no spikes in Ti and REE were observed during analysis. Perhaps the elevated Ti and REE are controlled by crystal defects in the zircon lattice, are not the result of equilibrium processes, or possibly represent non-Henry's law behavior in the incorporation of Ti and REE in zircon under some conditions. (e.g., Bindeman and Davis, 2000). The presence of this correlation is somewhat troubling for the use of Ti substitution in zircon as a thermometer, as it suggests that in some cases the REE content of zircon may have some effect on the Ti content.

5.3.2. Relation to MARID/PKP

The REE concentrations of the rutile-bearing Orapa (Botswana) suite of zircons are more highly variable than other suites of kimberlite zircons, including the chromite-bearing suite of megacrysts from the same pipe, yet have similar Ti content. The rutile-bearing suite may have formed under similar conditions to the chromite-bearing suite, but from a melt/fluid that was significantly more enriched (and variable) in REE content. The rutile-bearing suite of zircons from Orapa has REE compositions that overlap with MARID and PKP zircons compositions as well as typical megacryst compositions. At present, there is much more data on megacryst zircon from kimberlites than there is from zircon found in metasomatic xenoliths. Different Th/U systematics were thought to distinguish MARID zircons from megacrysts (Konzett et al., 1998). However, subsequent study has shown that MARID, PKP, and megacryst zircon form a continuum of Th/U compositions (Konzett et al., 2000). Zircons from the Orapa rutile nodule suite span the REE signatures of megacrysts and metasomatic zircons (Fig. 8d). Perhaps all zircon from kimberlite is metasomatic and differs only in the size of metasomatite in which it grows. Smaller regions of metasomatism may yield smaller and more chemically variable zircons in MARID or PKP assemblages.

Zircons from kimberlite allow the geochemical tools commonly applied to crustal zircon to be brought to bear on the mantle. These tools (oxygen and hafnium isotopes, REE systematics and now Ti-thermometry) have shown that these enigmatic crystals form in similar environments the world over, and preserve only subtle variations in geochemical signatures. Ti in zircon thermometry is in its infancy, and the possibility of a large pressure correction prohibits temperatures from this method to be literally interpreted with zircons from high and ultra-high pressure environments. Nonetheless, the limited range of Ti concentrations in these zircons suggests that the zircons form in similar pressure, temperature, and major element chemistry environments worldwide.

ACKNOWLEDGMENTS

We thank Brian Hess for careful sample preparation, grinding and polishing. Shawn Carlson (Ashton Mining of Canada Inc.) provided zircons from the Midwestern United Sates localities. E.B. Watson generously provided synthetic Ti-rich zircon for ion microprobe calibration. This research was supported by the U.S. National Science Foundation (EAR-0440343) and the U.S. Department of Energy (93ER14389). Wisc-SIMS is funded by the National Science Foundation (EAR-0319230, EAR05-16725, EAR05-09639). D.J.S. was supported by NSERC and De Beers.

APPENDIX A. SUPPLEMENTARY DATA

Supplementary data associated with this article can be found, in the online version, at doi:10.1016/j.gca.2007.04.031.

REFERENCES

Bell D. R. and Moore R. O. (2004) Deep chemical structure of the southern African mantle from kimberlite megacrysts. *S. African J. Geol.* **107**, 59–80.

Belousova E. A., Griffin W. L., O'Reilly S. Y. and Fisher N. I. (2002) Igneous zircon: trace element composition as an indicator of source rock type. *Contrib. Mineral. Petrol.* **143**, 602–622.

Belousova E. A., Griffin W. L. and Pearson N. J. (1998) Trace element composition and cathodoluminescence properties of southern African kimberlitic zircons. *Min. Mag.* **62**, 355–366.

Belousova E. A., Griffin W. L., Shee S. R., Jackson S. E. and O'Reilly S. Y. (2001) Two age populations of zircons from the Timber Creek kimberlites, Northern territory, Australia as determined by laser-ablation ICPMS analysis. *Austral. J. Earth Sci.* **48**, 757–766.

Bindeman I. N. and Davis A. M. (2000) Trace element partitioning between plagioclase and melt: investigation of dopant influence on partition behavior. *Geochim. Cosmochim. Acta* **64**, 2863–2878.

Boyd F. R., Dawson J. B. and Smith J. V. (1984) Granny-Smith diopside megacrysts from the kimberlites of the Kimberley area and Jagersfontein, South Africa. *Geochim. Cosmochim. Acta* **48**, 381–384.

Cannon W. and Mudrey, Jr., M. G. (1981) The potential for diamond-bearing kimberlite in Northern Michigan and Wisconsin. *U.S. Geol. Surv. Circular*, vol. 842, p. 15.

Carlson S. M. and Adams G. W. (1998) The diamondiferous Six-Pak ultramafic lamprophyre diatreme, Kenosha, Wisconsin. In Proc. Abstracts–Inst. Lake Sup. Geol., vol. 43, pp. 11–12.

Carlson S. M. and Floodstrand W. (1994) Michigan kimberlites and diamond exploration techniques. In Proc. Abstracts–Inst. Lake Sup. Geol., vol. 40, part 4, p. 15.

Corfu F., Hanchar J. M., Hoskin P. W. O. and Kinny, P. D. (2003) Atlas of zircon textures. In *Zircon, Rev. Mineral. Geochem.*, vol. 53 (eds. J. M. Hanchar and P. W. O. Hoskin). Mineralogical Society of America/Geochemical Society, pp. 469–500.

Davis G. L. (1977) The ages and uranium contents of zircons from kimberlites and associated rocks. *Carnegie Inst. Wash. Yearbook* **76**, 631–635.

Davis G. L., Sobolev N. V. and Khar'kiv A. D. (1980) New data on the age of Yakutian kimberlites obtained by the uranium-lead method on zircons. *Dok. Akad, Nauk SSSR* **254**, 175–179.

Dawson J. B., Hill P. G. and Kinny P. D. (2001) Mineral chemistry of a zircon-bearing, composite, veined and metasomatized upper-mantle peridotite xenolith from kimberlite. *Contrib. Mineral. Petrol.* **140**, 720–733.

Dawson J. B. and Smith J. V. (1977) MARID (Mica–amphibole–rutile–ilmenite–diopside) suite of xenoliths in kimberlite. *Geochim. Cosmochim. Acta* **41**, 309–323.

Deines P., Harris J. W., Robinson D. N., Gurney J. and Shee S. R. (1991) Carbon and oxygen isotope variation in diamond and graphite eclogites from Orapa, Botswana, and the nitrogen content of their diamonds. *Geochim. Cosmochim. Acta* **55**, 515–524.

Eiler J. M., Farley K. A., Valley J. W., Hofmann A. W. and Stolper E. M. (1996) Oxygen isotope constraints on the sources of Hawaiian volcanism. *Earth and Planet Sci. Lett.* **144**, 453–468.

Ferry J. M. and Watson E. B. (2006) New thermodynamic analysis and calibration of the Ti-in-zircon and Zr-in-rutile geothermometers. *Geol. Soc. Am. Abstr. Prog.* **38**, 243.

Fu B., Cavosie A. J., Clechenko C. C., Fournelle J. H., Kita N. T., Lackey J. S., Page F. Z., Wilde S. and Valley J.W. (2005) Ti-in-zircon thermometer: preliminary results. *Eos, Trans. AGU 86, Fall Meet.* Suppl., Abstract V41F-1538.

Garanin V. K., Kasimova F. I. and Melnikov F. P. (1993) Translated title: The temperature of formation of zircon and its paragenetic associations from the Mir kimberlite pipe. *Izvestiya VUZOV Geol. Explor.* **1**, 67–70, in Russian.

Griffin W. L., Pearson N. J., Belousova E., Jackson S. E., van Achterbergh E., O'Reilly S. Y. and Shee S. R. (2000) The Hf isotope composition of cratonic mantle: LAM-MC-ICPMS analysis of zircon megacrysts in kimberlites. *Geochim. Cosmochim. Acta* **64**, 133–147.

Gurney J. J., Jakob, W. R. O. and Dawson, J. B. (1979) Megacrysts from the Monastery kimberlite pipe, South Africa. In *The Mantle Sample: Inclusions in Kimberlites and Other Volcanics, Proceedings of the Second International Kimberlite Conference*, Vol. 2 (eds. F. R. Boyd and H. O. A. Meyer). American Geophysical Union.

Hanchar J. M. and Hoskin P. W. O. (2003) *Zircon–Reviews in Mineralogy and Geochemistry*, vol. 53, Mineralogical Society of America/Geochemical Society, p. 500.

Hamilton M. A., Pearson D. G., Stern R. A. and Boyd F. R. (1998) Constraints on MARID petrogenesis: SHRIMP II U-Pb zircon evidence for pre-eruptive metasomatism at Kamfersdam. *7th Int. Kimberlite Conf. Ext. Abstr.*, pp. 296–298.

Harrison T. M., Aikman A., Holden P., Walker A. M., McFarlane C., Rubatto D. and Watson E. B. (2005) Testing the Ti-in-zircon thermometer. *Eos, Trans. AGU 86, Fall Meet.* Suppl., Abstract V41F-1540.

Holden P., Aikman A., Ireland T. R. and Heiss J. (2005) Does Ti record the crystallization temperature of zircon? *Eos, Trans. AGU 86, Fall Meet.* Suppl., Abstract V41F-1539.

Hoskin P. W. O. and Ireland T. R. (2000) Rare earth element chemistry of zircon and its use as a provenance indicator. *Geology* **28**, 627–630.

Kinny P. D., Compston W., Bristow J. W. and Williams I. S. (1989) Archaean mantle xenocrysts in a Permian kimberlite: two generations of kimberlitic zircon in Jwaneng DK2, southern Botswana. In *Kimberlites and Related Rocks,* vol. 14 (eds. J. Ross, L. Jaques, J. Ferguson, D. H. Green, S. O'Reilly, R. Danchin, and A. Janse), Geological Society of Australia, pp. 833–842.

Kinny P. D. and Dawson J. B. (1992) A mantle metasomatic injection event linked to late Cretaceous Kimberlite magmatism. *Nature* **360**, 726–728.

Kinny P. D., Griffin B. J. and Brakhfogel F. F. (1995) SHRIMP U–Pb ages of perovskite and zircon from Yakutian kimberlites. In *Proceedings of the Sixth International Kimberlite Conference: dedicated to the memory of Henry Meyer* (eds. N. V. Sobolev and R. H. Mitchell), p. 275.

Kita N. T., Ikeda Y., Togashi S., Liu Y. Z., Morishita Y. and Weisberg M. K. (2004) Origin of ureilites inferred from a SIMS oxygen isotopic and trace element study of clasts in the Dar al Gani 319 polymict ureilite. *Geochim. Cosmochim. Acta* **68**, 4213–4235.

Konzett J., Armstrong R. A. and Gunther D. (2000) Modal metasomatism in the Kaapvaal craton lithosphere: constraints on timing and genesis from U–Pb zircon dating of metasomatized peridotites and MARID-type xenoliths. *Contrib. Mineral. Petrol.* **139**, 704–719.

Konzett J., Armstrong R. A., Sweeney R. J. and Compston W. (1998) The timing of MARID metasomatism in the Kaapvaal mantle: An ion probe study of zircons from MARID xenoliths. *Earth Planet. Sci. Lett.* **160**, 133–145.

Kresten P., Fels P. and Berggren G. (1975) Kimberlitic Zircons–possible aid in prospecting for Kimberlites. *Mineralium Deposita* **10**, 47–56.

Mattey D., Lowry D. and Macpherson C. (1994) Oxygen isotope composition of mantle peridotite. *Earth and Planet Sci. Lett.* **128**, 231–241.

McGee E. S. and Hearn, Jr., B. C., (1983). Lake Ellen kimberlite, Michigan, U.S.A. U.S. Geological Survey Open-File Report OF 83-0156, p. 24.

Moore R. O. (1992) Trace element geochemistry of ilmenite megacrysts from the Monastery kimberlite, South Africa. *Lithos* **29**, 1–18.

Nixon P. H. and Boyd F. R. (1973) The discreet nodule association in kimberlites from northern Lesotho. In *Lesotho Kimberlites* (ed. P. H. Nixon). Lesotho National Development Corporation, pp. 67–75.

Pollack H. N. and Chapman D. S. (1977) On the regional variation of heatflow, geotherms and lithospheric thickness. *Tectonophysics* **38**, 279–296.

Schmitz M. D. and Bowring S. A. (2003) Ultrahigh-temperature metamorphism in the lower crust during Neoarchean Ventersdorp rifting and magmatism, Kaapvaal Craton, southern Africa. *Geol. Soc. Am. Bull.* **115**, 533–548.

Schulze D. J. (1987) Megacrysts in alkaline volcanic rocks. In *Mantle Xenoliths* (ed. P. H. Nixon). Wiley, pp. 433–451.

Schulze D. J. (1990) Silicate-bearing rutile-dominated nodules from South African kimberlites: Metasomatized cumulates. *Amer. Mineral.* **75**, 97–104.

Schulze D. J., Valley J. W., Bell D. R. and Spicuzza M. J. (2001) Oxygen isotope variations in Cr-poor megacrysts from kimberlite. *Geochim. Cosmochim. Acta* **65**, 4375–4384.

Shannon R. and Prewitt C. (1969) Effective ionic radii in oxides and fluorides. *Acta Crystal. B* **25**, 925–946.

Skinner E. (1989) Contrasting group I and group II kimberlite petrology: towards a genetic model for kimberlites. In *Kimberlites and Related Rocks, vol. 1. Their Composition, Occurrence, Origin and Emplacement* (ed. J. A. Ross). Blackwell Scientific Publishing, pp. 528–544.

Smith C. B. (1983) Pb, Sr and Nd isotopic evidence for sources of southern African Cretaceous Kimberlites. *Nature* **304**, 51–54.

Smith C. B., Schulze D. J., Bell D. R. and Viljoen K. S. (1995) Bearing of the sub-calcic, Cr-poor megacryst suite on kimberlite petrogenesis and lithospheric structure. In *Extended Abstracts: Sixth International Kimberlite Conference*, pp. 546–548.

Spetsius Z. V., Belousova E. A., Griffin W. L., O'Reilly S. Y. and Pearson N. J. (2002) Archean sulfide inclusions in Paleozoic zircon megacrysts from the Mir kimberlite, Yakutia: implications for the dating of diamonds. *Earth Planet. Sci. Lett.* **199**, 111–126.

Valley J. W. (2003) Oxygen isotopes in zircon. In *Zircon, Rev. Mineral. Geochem. Vol. 53* (eds. J. M. Hanchar and P. W. O. Hoskin). Mineralogical Society of America/Geochemical Society, pp. 343–385.

Valley J. W., Kinny P. D., Schulze D. J. and Spicuzza M. J. (1998) Zircon megacrysts from kimberlite: oxygen isotope variability among mantle melts. *Contrib. Mineral. Petrol.* **133**, 1–11.

Valley J. W., Kitchen N., Kohn M. J., Niendorf C. R. and Spicuzza M. J. (1995) UWG-2, a garnet standard for oxygen isotope ratios: strategies for high precision and accuracy with laser heating. *Geochim. Cosmochim. Acta* **59**, 5223–5231.

Watson E. B. and Harrison T. M. (2005) Zircon thermometer reveals minimum melting conditions on earliest Earth. *Science* **308**, 841–844.

Watson E. B., Wark D. A. and Thomas J. B. (2006). Crystallization thermometers for zircon and rutile. *Contrib. Mineral. Petrol.* **151**, 413–433.

Wiedenbeck M., Hanchar J. M., Peck W. H., Sylvester P., Valley J., Whitehouse M., Kronz A., Morishita Y., Nasdala L., Fiebig J., Franchi I., Girard J. P., Greenwood R. C., Hinton R., Kita N., Mason P. R. D., Norman M., Ogasawara M., Piccoli R., Rhede D., Satoh H., Schulz-Dobrick B., Skar O., Spicuzza M. J., Terada K., Tindle A., Togashi S., Vennemann T., Xie Q. and Zheng Y. F. (2004) Further characterization of the 91500 zircon crystal. *Geostand. Geoanal. Res.* **28**, 9–39.

Zartman R. E. and Richardson S. H. (2005) Evidence from kimberlitic zircon for a decreasing mantle Th/U since the Archean. *Chem. Geol.* **220**, 263–283.

Zhao D. G., Essene E. J. and Zhang Y. X. (1999) An oxygen barometer for rutile–ilmenite assemblages: oxidation state of metasomatic agents in the mantle. *Earth Planet. Sci. Lett.* **166**, 127–137.

Associate editor: James Farquhar